

## Preliminary Microstructural and Microscratch Results of Ni-Cr-Fe and Cr<sub>3</sub>C<sub>2</sub>-NiCr Coatings on Magnesium Substrate

**B Istrate<sup>1</sup>, C Munteanu<sup>1\*</sup>, S Lupescu<sup>1</sup>, M Benchea<sup>1</sup> and P Vizureanu<sup>2</sup>**

<sup>1</sup> “Gheorghe Asachi” Technical University of Iasi, Faculty of Mechanical Engineering, 43 “D. Mangeron” Street, 700050, Iasi, Romania

<sup>2</sup> “Gheorghe Asachi” Technical University of Iasi, Faculty of Material Science and Engineering, 61-63 “D. Mangeron” Street, 700050, Iasi, Romania

E-mail: cornelmun@gmail.com

**Abstract.** Thermal coatings have a large scale application in aerospace and automotive field, as barriers improving wear mechanical characteristics and corrosion resistance. In present research, there have been used two types of coatings, Ni-Cr-Fe, respectively Cr<sub>3</sub>C<sub>2</sub>-NiCr which were deposited on magnesium based alloys (pure magnesium and Mg-30Y master alloy). There have been investigated the microstructural aspects through scanning electronic microscopy and XRD analysis and also a series of mechanical characteristics through microscratch and indentation determinations. The results revealed the formation of some adherent layers resistant to the penetration of the metallic indenter, the coatings did not suffer major damages. Microstructural analysis highlighted the formation of Cr<sub>3</sub>C<sub>2</sub>, Cr<sub>7</sub>C<sub>3</sub>, Cr<sub>3</sub>Ni<sub>2</sub>, Cr<sub>7</sub>Ni<sub>3</sub>, FeNi<sub>3</sub>, Cr-Ni phases. Also, the apparent coefficient of friction for Ni-Cr-Fe coatings presents superior values than Cr<sub>3</sub>C<sub>2</sub>-NiCr coatings.

### 1. Introduction

Thermal coatings represent some special coatings processes, which has seen an accelerated development in the last decades, especially in automotive, naval, aerospace domains, like: turbine blades, cylinders, pistons, valves, in order to improve wear resistance, corrosion resistance and lifetime of the machine part [1–3]. The most common thermal deposition techniques are APS and HVOF, but there are also other coatings methods like: flame spraying, wire arc spraying, PLD etc [4–9]. Coatings obtained by plasma jet deposition (APS) with formation of Ni, Cr ceramic layers are among used materials in mechanical applications [10]. The main disadvantage of these coatings could represent the isolated inhomogeneity, micro-cracks and residual stresses. These stresses occur during cooling process of thermal spraying [11].

Mayrhofer et al. highlighted the wear resistance improvement of steel substrates by using Cr<sub>3</sub>C<sub>2</sub> stabilized with NiCr layers in comparison with WC coatings [12]. It has been also shown that Cr<sub>3</sub>C<sub>2</sub>-NiCr coatings present comparable wear with tungsten carbide, but it has superior oxidation resistance [2]. Varies et al. studied the fatigue resistance improvement Cr<sub>3</sub>C<sub>2</sub> based coatings by performing some kinetic energy layers and special treatments [13]. The researchers showed that the coatings which contain iron, improve the layers ability to make diffusion with base material being also cheaper and less pollutant with the environment than Co and Ni based coatings [14,15].

In the present paper, authors deposited two types of plasma jet coatings (Cr<sub>3</sub>C<sub>2</sub>-NiCr and Ni-Cr-Fe) on magnesium alloys substrate (Pure Mg and Mg-30Y master alloy). It have been used these based



materials due their applicability in automotive and aerospace domains. Kula et al. highlighted that the presence of Yttrium in magnesium alloys lead to hardness and ductility improvement [16].

There have been performed morphological analyses of deposited layers, phase identification using XRD determination and also identification of some mechanical characteristics using scratch and indentation method.

## 2. Materials and methods

Ni-Cr-Fe, respectively  $\text{Cr}_3\text{C}_2$ -NiCr coatings were obtained using atmospheric plasma spray facility (SPRAYWIZARD-9MCE, Sultzer-Metco, USA/ 9MB spraying gun) with typically particle size between 10-90 microns. The substrates of these coatings used in this present research were pure magnesium and a Mg-30Y master alloy (HB New Material, Changsta China). In table 1 are highlighted the technological parameters used for the coating process.

Morphological and microstructure have been determined using a LFD (large field detector), respectively dual BSD (backscattered detector) on a scanning electron microscope SEM Quanta 200 3D DUAL BEAM. For phase analysis, XRD analysis was carried out using an X'Pert Pro MPD diffractometer, with a copper X-ray tube –  $\text{K}\alpha$ : 1.54 Å, in 2Theta scanning range of 20°-90°. Apparent coefficient of friction, hardness and elastic modulus were measured using CETR UMT-2 Tribometer. Micro-scratch analysis parameters consist in: a constant load of 5N for a distance of 4 mm, for a single determination, on a flat sample of 20mm x10mm sample. Also, for the indentation determination, there were performed three determinations for each sample with a constant load of 5 N and using a metallic indenter.

**Table 1.** Technological parameters used for coating process.

Powder	Gun	Ar		H <sub>2</sub>		Electric		Powder feeder 9MP			Spray distance (inch)
		Pressure (psig)	Gas flow (SCFH)	Pressure (psig)	Gas flow (SCFH)	DC (A)	DC (V)	Carrier gas flow (SCFH)	Air Pressure (psig)	Rate (lb/h)	
Cr <sub>3</sub> C <sub>2</sub> -NiCr coating	9MB	75	111	50	10	500	60-70	13.5	20	5.5	2.25
Ni-Cr-Fe coating		75	90	50	20	500	70-80	13.5	20	4	9

## 3. Results and discussions

### 3.1. Structural analysis

**3.1.1. Scanning electron microscopy.** Microstructure and morphology aspects of the ceramic coatings are presented in figures 1-4. In figure 1 (a-f) is presented the specific deposition aspects of APS method of a  $\text{Cr}_3\text{C}_2$ -NiCr, respectively Ni-Cr-Fe based coatings.

These ceramic layers have on the surface an average roughness with the presence of some small unmolded particle, few micropores and some microcracks, due the recovery process of thermal deposition. Different scale images present that in both cases an adherent coating with the substrate.

In figures 2-4 are shown cross-section images (a-f) for  $\text{Cr}_3\text{C}_2$ -NiCr / Ni-Cr-Fe layers. Ceramic coatings have the appearance of columnar grains called "splats", due the layer by layer spraying technique and having an average thickness of the splat of 3 microns (figure 4).

The average thickness of coatings are presented in figure 2(a, e), respectively in figure 3 (a, d) which is aproximatively 200 µm for  $\text{Cr}_3\text{C}_2$ -NiCr coating and respectively 150 µm for Ni-Cr-Fe coating.

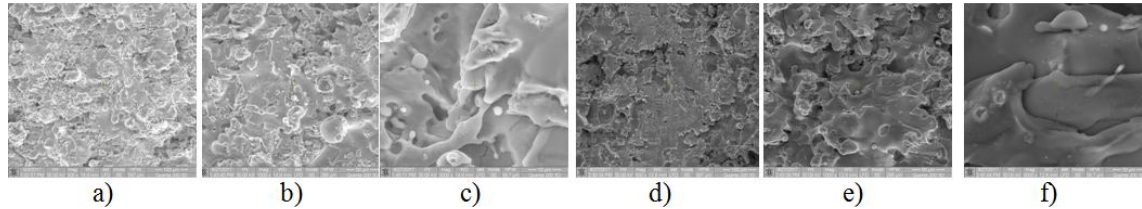


**Figure 1.** Surface SEM images for  $\text{Cr}_3\text{C}_2$ -NiCr coating: a), b), c); Ni-Cr-Fe coating: d), e), f).

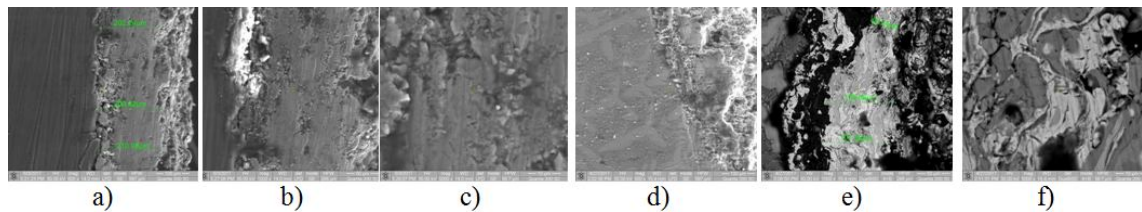


**Figure 2.** Cross-section SEM images for  $\text{Cr}_3\text{C}_2$ -NiCr on pure Mg substrate: a), b), c); Mg-30Y substrate: d), e), f).

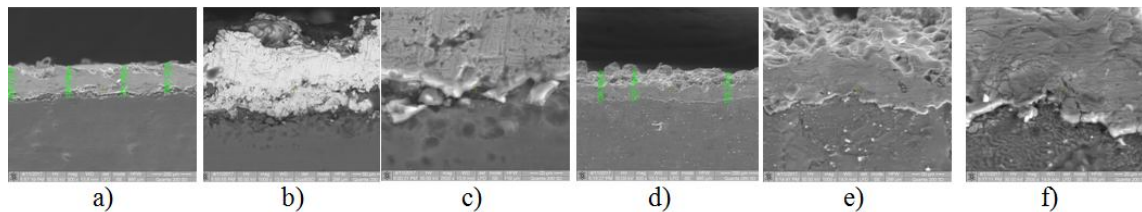


**Figure 3.** Cross-section SEM images for Ni-Cr-Fe on pure Mg substrate: a), b), c); Mg-30Y substrate: d), e), f).

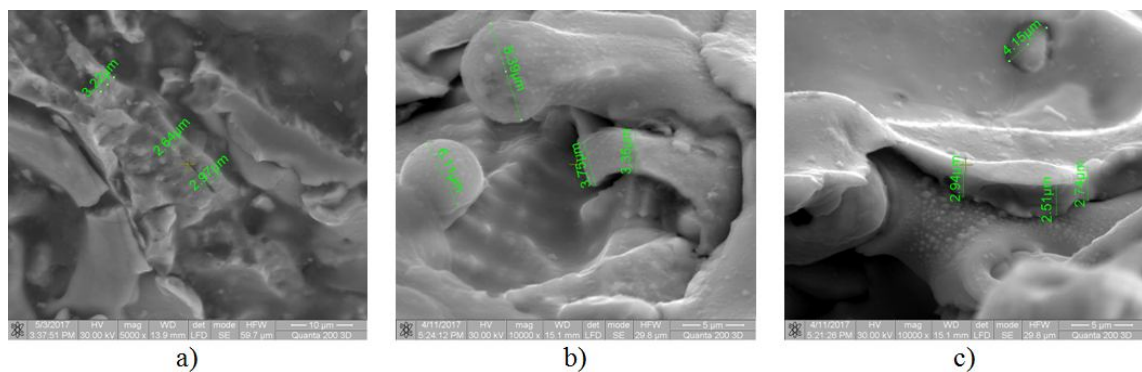


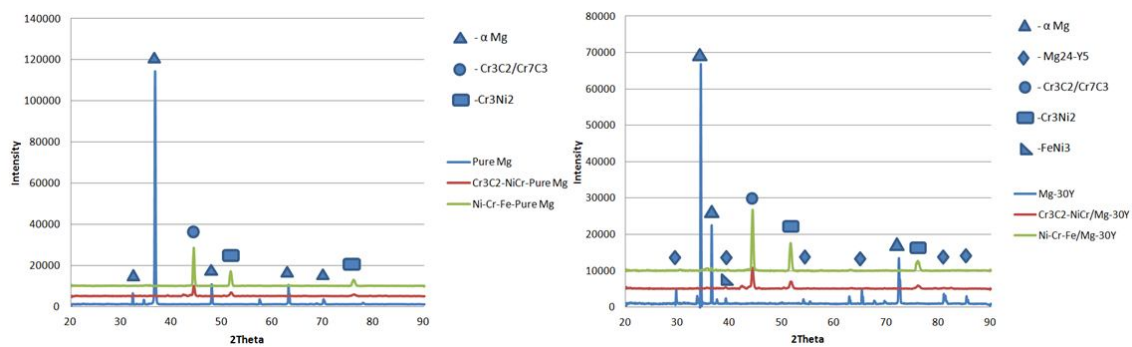
**Figure 4.** Aspects of spraying results: a)  $\text{Cr}_3\text{C}_2$ -NiCr; b),c) Ni-Cr-Fe coating.

**3.1.2. XRD analysis.** XRD diffraction analyses are shown in Figure 5. The diffraction analysis highlighted Cr-based compounds:  $\text{Cr}_3\text{C}_2$ ,  $\text{Cr}_7\text{C}_3$ ,  $\text{Cr}_3\text{Ni}_2$ ,  $\text{Cr}_{0.1}\text{Ni}_{0.9}$ ,  $\text{Cr}_7\text{Ni}_3$  having both orthorhombic and tetragonal crystal structure.

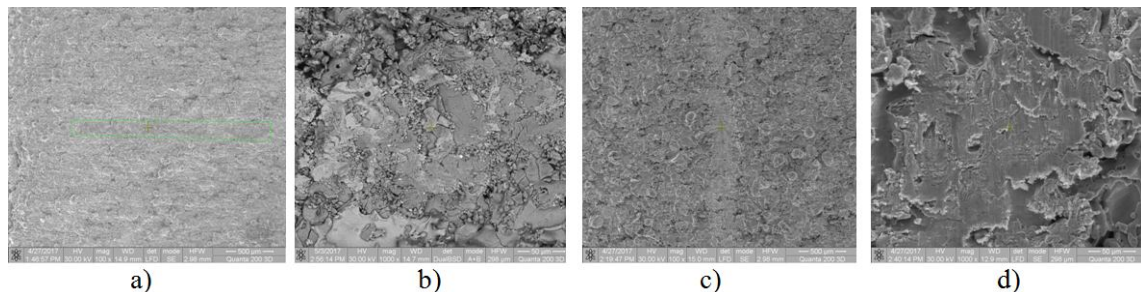
For the coatings,  $\text{Cr}_3\text{C}_2$  and  $\text{Cr}_7\text{C}_3$  are the predominant phases around at  $44.22^\circ$   $2\theta$  angle.  $\text{Cr}_3\text{Ni}_2$  and  $\text{FeNi}_3$  are the minority diffraction peaks of the coatings around  $51.67^\circ$   $2\theta$  angle and  $76.24^\circ$   $2\theta$  angle, with a tetragonal, respectively cubic structure. Base materials consist three types of compounds:  $\alpha$ -Mg (hexagonal structure) and MgY, respectively  $\text{Mg}_{24}\text{Y}_5$  (cubic structure). Lattice parameters of all identified compounds are shown in table 2.

**Table 2.** Lattice parameters of  $\text{Cr}_3\text{C}_2$ -NiCr / Ni-Cr-Fe coatings / Base materials (Pure Mg / Mg-30Y).

	Compound	Space Group	Crystal system	a (Å)	b (Å)	c (Å)	$\alpha$ (°)	$\beta$ (°)	$\gamma$ (°)	Cell volume (10 <sup>6</sup> pm <sup>3</sup> )
Cr3C2-NiCr coating	Cr <sub>3</sub> C <sub>2</sub>	Pnam	Orthorhombic	5,5250	11,4680	2,8266	90	90	90	179,10
	Cr <sub>7</sub> C <sub>3</sub>	Pnma	Orthorhombic	4,5260	7,0100	12,1420	90	90	90	385,23
	Cr <sub>3</sub> Ni <sub>2</sub>	P42/mnm	Tetragonal	8,8200	8,8200	4,5800	90	90	90	356,29
	Cr <sub>7</sub> Ni <sub>3</sub>	P42/mnm	Tetragonal	8,7100	8,7100	4,4900	90	90	90	340,63
	Cr <sub>0,1</sub> Ni <sub>0,9</sub>	P-3m1E	Cubic	3,5350	3,5350	3,5350	90	90	90	44,17
Ni-Cr-Fe coating	Cr <sub>1,12</sub> Ni <sub>2,88</sub>	Fm-3m	Cubic	3,5400	3,5400	3,5400	90	90	90	44,36
	FeNi <sub>3</sub>	Fm-3m	Cubic	3,5556	3,5556	3,5556	90	90	90	44,95
	Cr <sub>0,1</sub> Ni <sub>0,9</sub>	Fm-3m	Cubic	3,5350	3,5350	3,5350	90	90	90	44,17
Pure Mg / Mg-30Y	Mg	P63/mmc	Hexagonal	3,2088	3,2088	5,2099	90	90	120	46,46
	MgY	Pm-3m	Cubic	3,7900	3,7900	3,7900	90	90	90	54,44
	Mg <sub>24</sub> Y <sub>5</sub>	I-43m	Cubic	11,2500	11,2500	11,2500	90	90	90	1423,83

**Figure 5.** XRD patterns of  $\text{Cr}_3\text{C}_2$ -NiCr / Ni-Cr-Fe coatings.

**3.1.3. Scratch and micro-indentation analysis.** Figure 6 presents SEM images of scratch test of  $\text{Cr}_3\text{C}_2$ -NiCr coatings (a, b), respectively Ni-Cr-Fe coatings. The apparent coefficient of friction for the  $\text{Cr}_3\text{C}_2$ -NiCr layer is in the range of 0.55. Same analyses were carried out for the second layer, respectively Ni-Cr-Fe, which presented an apparent coefficient of friction around 1.25.

**Figure 6.** SEM images of scratch test for  $\text{Cr}_3\text{C}_2$ -NiCr coatings (a,b), Ni-Cr-Fe coatings (c,d).

SEM images showed adherent layers without removing to the base material. It have been observe a small number of microcracks in both of the coatings, resulting less fragile layers. Coatings present similar values of the stiffness between 3.589 and 3.953  $\text{N}/\mu\text{m}$ . The results of microindetation test have shown a depth of between 6.15  $\mu\text{m}$  and 16.33  $\mu\text{m}$  for  $\text{Cr}_3\text{C}_2$ -NiCr layer, respectively 8.46  $\mu\text{m}$  and 18.91  $\mu\text{m}$  for the second, without fracturing. It can be concluded that both coatings have high



resistance to fracturing, a fact confirmed by hardness values and coefficient of friction apparently values presented in table 3 and figure 7. Also the hardness is influenced by the substrate, Yttrium has superior behavior in magnesium alloys [14].

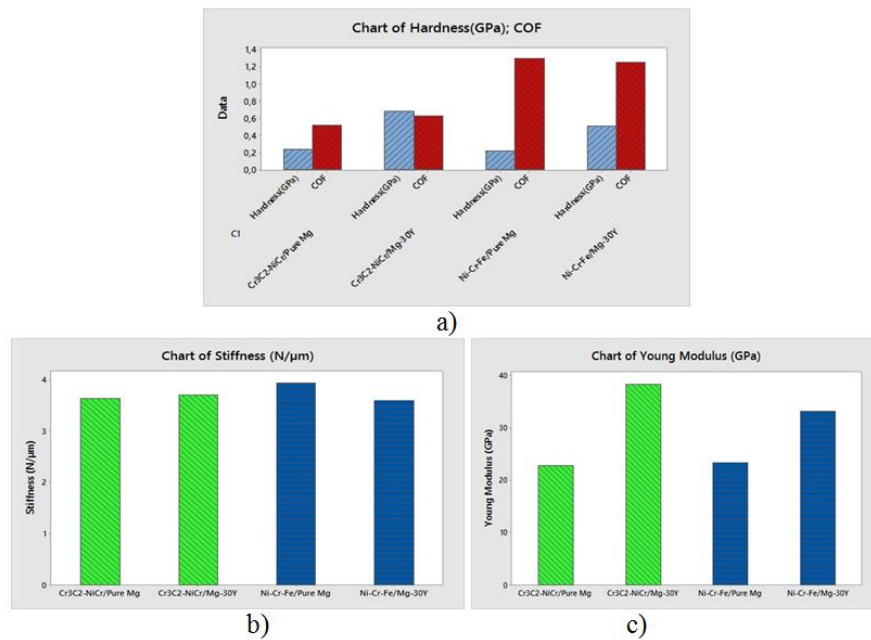


**Figure 7.** Some mechanical characteristics obtained by scratch and microindentation analysis: a) Hardness/COF; b) Stiffness; c) Young modulus.

Young modulus is influenced by the substrate characteristics. The coatings performed on pure magnesium substrate show similar values between 22.79 GPa and 23.37 GPa and also the coatings deposited on Mg-30Y revealed higher values of elastic modulus between 33.17 GPa and 38.34 GPa.

**Table 3.** Some mechanical properties of Cr3C2-NiCr / Ni-Cr-Fe coatings on Pure Mg, respectively Mg-30Y substrate.

	COF	Hardness (GPa)	Young Modulus (GPa)	Stiffness(N/μm)
Cr3C2-NiCr / Pure Mg	0.515	0.239	22.795	3.630
Cr3C2-NiCr / Mg-30Y	0.629	0.683	38.343	3.701
Ni-Cr-Fe / Pure Mg	1.298	0.217	23.375	3.935
Ni-Cr-Fe / Mg-30Y	1.253	0.513	33.172	3.589

#### 4. Conclusions

The aim of this research was to investigate the morphological appearance, X-ray diffraction, micro-scratch and micro-indentation aspects on Cr3C2-NiCr / Ni-Cr-Fe coatings on Pure Mg, respectively Mg-30Y substrate. These coatings confirm the presence of “splats” particles with an average size of 3 microns. Also, on the surface of the coatings it has been observed typically plasma deposition morphology like, few microcracks, unmolded particles etc. X-Ray analysis showed the presence Cr-based compounds: Cr3C2, Cr7C3, Cr3Ni2, Cr0.1Ni0.9, Cr7Ni3 having both orthorhombic and tetragonal crystal structure as predominant phase. Also was identified as secondary phase Cr3Ni2 and FeNi3 with a crystal structure of tetragonal and cubic type. Young modulus is influenced by the substrate

characteristics. The coatings performed on pure magnesium, respectively Mg-30Y substrate show similar values. Also, the apparent COF of Cr<sub>3</sub>C<sub>2</sub>-NiCr is lower than COF of Ni-Cr-Fe coatings. Research will continue with future experiments in order to evaluate the coatings characteristics for different types of applications.

## References

- [1] Lu Z, Myoung S W, Kim E H, Lee J H and Jung Y G 2014 *Mater. Today Proc.* **1** 35–43
- [2] Matikainen V, Bolelli G, Koivuluoto H, Sassatelli P, Lusvarghi L and Vuoristo P 2017 Sliding wear behaviour of HVOF and HVOF sprayed Cr<sub>3</sub>C<sub>2</sub>-based coatings *Wear* 0–1
- [3] Suarez M, Bellayer S, Traisnel M, Gonzalez W, Chicot D, Lesage J, Puchi-Cabrera E S and Staia M H 2008 *Surf. Coatings Technol.* **202** 4566–71
- [4] Avram P, Imbrea M S, Istrate B, Strugaru S I, Benchea M and Munteanu C 2014 *Indian J. Eng. Mater. Sci.* **21**
- [5] Sadeghimeresht E, Markocsan N and Nylén P 2016 Surface & Coatings Technology Microstructural characteristics and corrosion behavior of HVOF- and HVOF-sprayed Fe-based coatings *Sct*
- [6] Berger L M 2015 *Int. J. Refract. Met. Hard Mater.* **49** 350–64
- [7] Rațoi M, Dascălu G, Stanciu T, Gurlui S O, Stanciu S, Istrate B, Cimpoesu N and Cimpoesu R 2014 *Preliminary results of FeMnSi+Si(PLD) alloy degradation* **638**
- [8] Perju M C, Vizureanu P 2014 REV. CHIM. (Bucharest) 65(6) 694-696
- [9] Cimpoesu N, Stanciu S, Vizureanu P, Cimpoesu R, Achitei D C, Ionita I 2014 *Journal of Mining and Metallurgy* **50**(1) 69-76
- [10] Gariboldi E, Rovatti L, Lecis N, Mondora L and Mondora G A 2016 *Surf. Coatings Technol.* **305** 83–92
- [11] Tsui Y C and Clyne T W 1997 *Thin Solid Films* **306** 23–33
- [12] Mayrhofer E, Janka L, Mayr W P, Norpoth J, Rodriguez Ripoll M and Gröschl M 2015 *Surf. Coatings Technol.* **281** 169–75
- [13] Varis T, Suhonen T, Caloni O, ?uban J and Pietola M 2016 *Surf. Coatings Technol.* **305** 123–31
- [14] Liu W-H, Shieu F-S and Hsiao W-T 2014 *Surf. Coatings Technol.* **249** 24–41
- [15] Wang S, Cheng J, YI S-H and KE L 2014 *Trans. Nonferrous Met. Soc. China* **24** 146–51
- [16] Kula A, Jia X, Mishra R K and Niewczas M 2017 *Int. J. Plast.* **92** 96–121